Numerical simulation of electromagnetic scattering by morphologically complex objects

Janna M. Dlugach*, Michael I. Mishchenko**

*Main Astronomical Observatory of the National Academy of Sciences of Ukraine, Kyiv, Ukraine
**NASA Goddard Institute for Space Studies, New York, USA

Radiation mechanisms of astrophysical objects: classics today
21 – 25 September, 2015, St.Petersburg. Russia

I. Methodology

$\mathbf{I}_{sca} \propto \mathbf{F}\mathbf{I}_{inc.}$ – transformation of the Stokes vector of the incident radiation to the Stokes vector of the scattered radiation.

$$\mathbf{I} = \begin{bmatrix} I \\ Q \\ U \\ V \end{bmatrix}$$

The case of macroscopically isotropic and mirror-symmetric medium:

$$\mathbf{F} = \begin{bmatrix} a_1(\theta) & b_1(\theta) & 0 & 0 \\ b_1(\theta) & a_2(\theta) & 0 & 0 \\ 0 & 0 & a_3(\theta) & b_2(\theta) \\ 0 & 0 & -b_2(\theta) & a_4(\theta) \end{bmatrix}$$

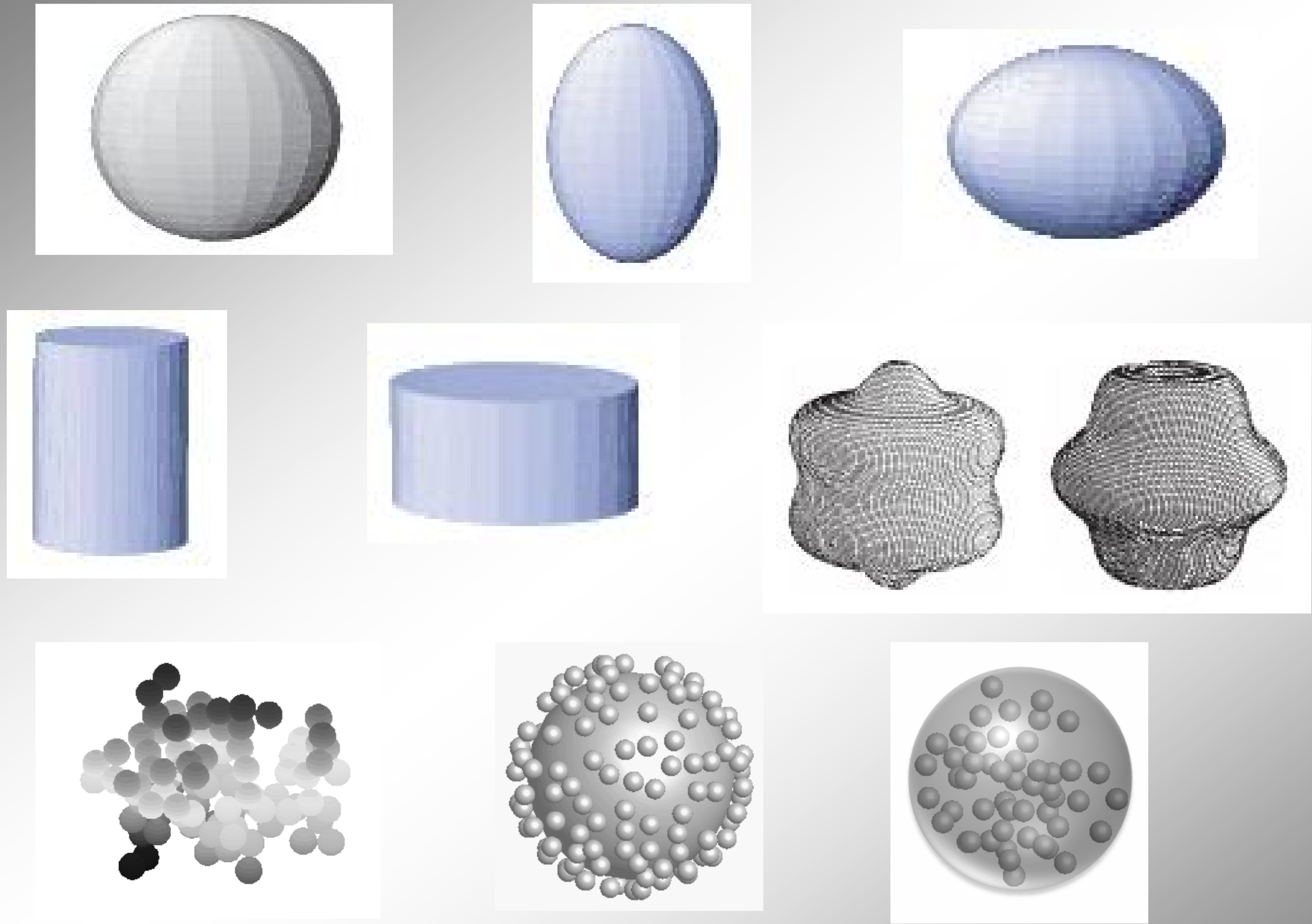

Shapes of considered particles.

Sparse plane-parallel macroscopically isotropic and mirror-symmetric medium

$$\mu \frac{\mathrm{d}\mathbf{I}(\tau,\mu,\varphi)}{\mathrm{d}\tau} = -\mathbf{I}(\tau,\mu,\varphi) + \frac{\omega(\tau)}{4\pi}\int_0^{2\pi} d\varphi' \int_{-1}^{1} d\mu' \widetilde{\mathbf{Z}}(\tau;\mu,\varphi;\mu',\varphi')\mathbf{I}(\tau,\mu',\varphi'),$$

$$\mathbf{I}(0,\mu,\varphi) = \delta(\mu-\mu_0)\delta(\varphi-\varphi_0)\mathbf{I}_0,$$

$$\mathbf{I}(\tau_0,-\mu,\varphi) = 0.$$

$$\mathbf{I}(-\mu,\varphi) = \frac{1}{\pi}\mu_0 \mathbf{R}(\mu,\mu_0,\varphi-\varphi_0)\mathbf{I}_0.$$

In the case of unpolarized incident radiation:

$$I(-\mu,\varphi) = \mu_0 R_{11}(\mu,\mu_0,\varphi-\varphi_0),$$

$$Q(-\mu,\varphi) = \mu_0 R_{21}(\mu,\mu_0,\varphi-\varphi_0), \qquad P = -Q/I.$$

II. The effect of particle shape on microphysical properties of aerosols retrieved from spectropolarimetric observations

Observational data: spectropolarimetric observations at the center of the Jovian disk in the phase angle range 0º $< \alpha <$ 11º (Morozhenko (1976)) and the spectrophotometric data Woodman et al. (1979) at a phase angle 2º (Woodman et al. (1979)) .

Aerosol models: spheres, randomly oriented oblate and prolate spheroids, and finite circular cylinders. Particle polydispersity is characterized by a simple gamma size distribution.

Models of the upper Jovian atmosphere: A) a semi-infinite homogeneous layer composed of uniformly mixed gas and cloud particles, and **B)** a two-layer atmosphere in which a gas layer of optical thickness τ_g overlays a semi-infinite homogeneous layer composed of a uniform mixture of gas and cloud particles.

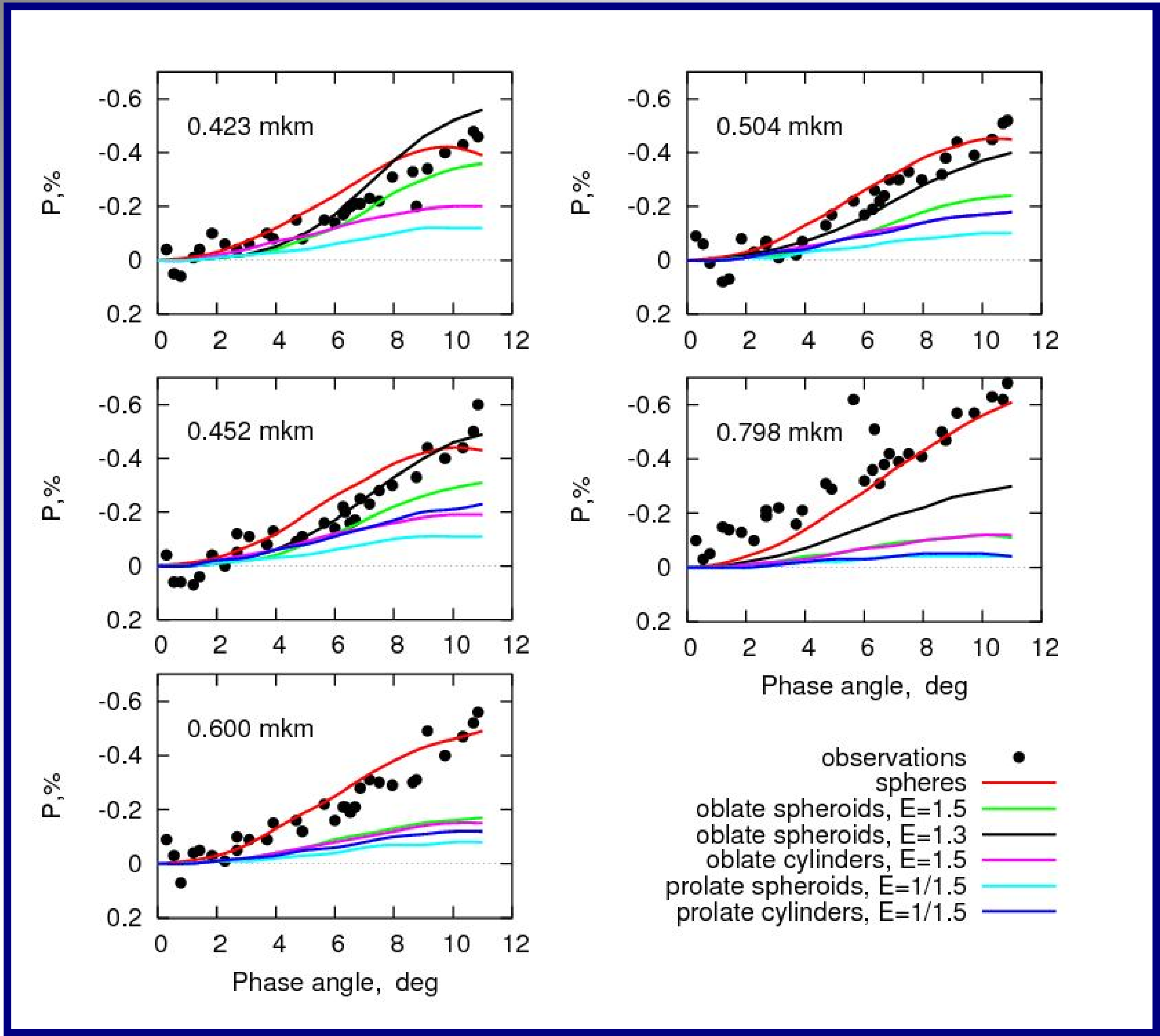

Phase angle dependence of the degree of linear polarization for the center of the Jovian disk.

Best-fit microphysical parameter values for various particle models (Mishchenko (1990), Dlugach&Mishchenko (2004, 2005))

Shape	E	m_R	r_{eff}, μm	v_{eff}	Model
Spheres	1.0	1.386	0.385	0.45	A
Oblate spheroids	1.3	1.45	0.35	0.40	B
Oblate spheroids	1.5	1.52	0.40	0.35	B
Prolate spheroids	1.3	1.50	0.35	0.30	B
Prolate spheroids	1.5	1.54	0.90	0.30	A
Oblate cylinders	1.3	1.43	0.47	0.40	B
Prolate cylinders	1.3	1.49	0.60	0.40	B

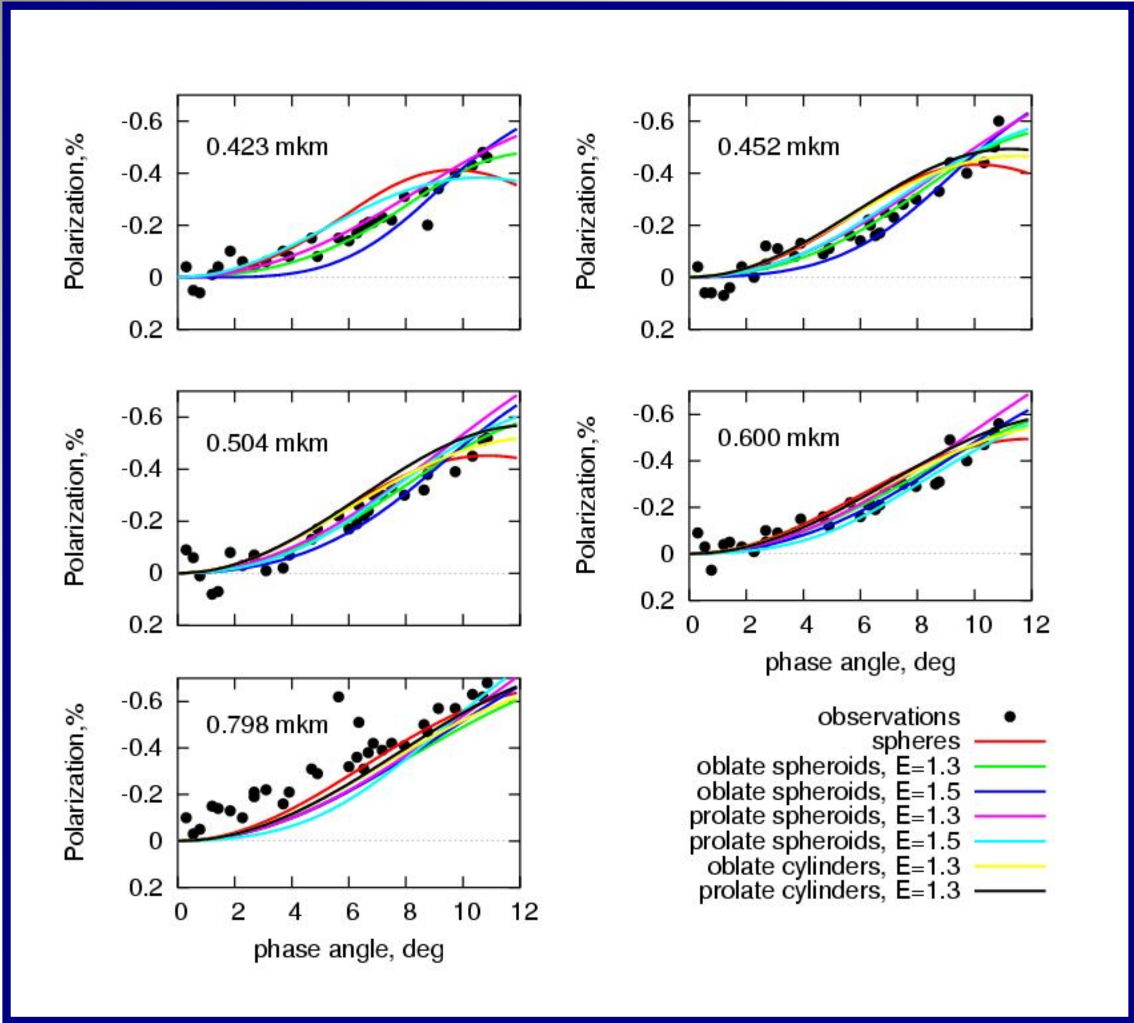

Phase angle dependence of the degree of linear polarization for the center of the Jovian disk.

Conclusion

- Specific choice of particle shape in model computations can affect significantly the retrieval of cloud particle parameters from spectropolarimetric data. Even weak asphericity of the assumed particle shape causes significant changes in the values of the particle microphysical characteristics as compared to that retrieved with the spherical particle model.

- The lack of a priori information on the actual particle shape limits our ability to obtain reliable estimates of particle microphysical parameters based on analyses of polarimetric measurements taken at a narrow range of phase angles.

III. Analysis of the results of radar polarimetry of Saturn's rings

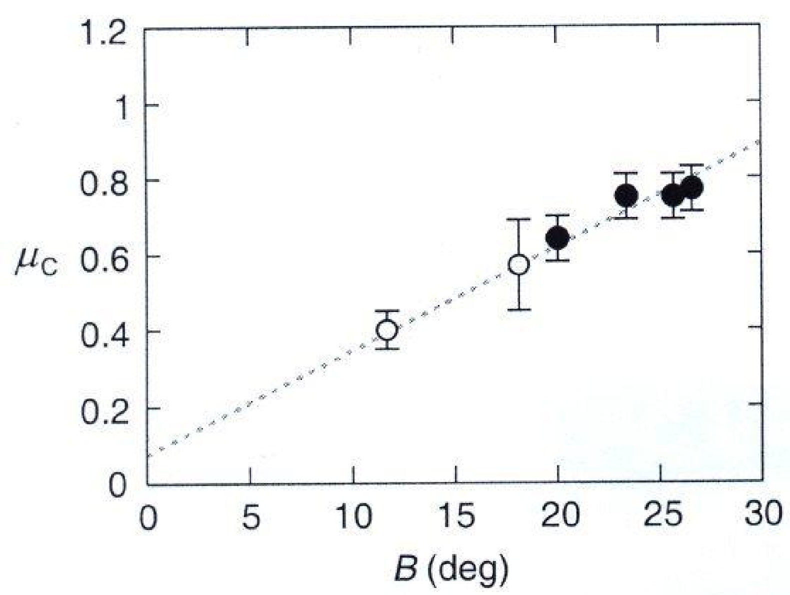

Variation of the average circular polarization ratio μ_C with ring opening angle *B* for the A and B rings of Saturn based on all available radar data at 12.6 cm.

$$\mu_{\mathrm{C}} = \frac{\widetilde{I}_{sh}}{\widetilde{I}_{oh}} = \frac{R_{11}^{1} + R_{44}^{1} + 2R_{11}^{\mathrm{M}} + 2R_{44}^{\mathrm{M}}}{R_{11}^{1} - R_{44}^{1} + R_{11}^{\mathrm{M}} + R_{22}^{\mathrm{M}} - R_{33}^{\mathrm{M}} - R_{44}^{\mathrm{M}}}.$$

Adopted model of the ring system: vertically and horizontally homogeneous plane-parallel layer of random particulate medium of an arbitrary optical thickness, composed of randomly oriented nonspherical particles with the refractive index $m = 1.78 + 0.003i$ and power law size distribution.

Analysis of radar measurements of the polarization ratio involves the following:

1. the computation of the single-scattering properties of the ring particles;
2. the computation of the diffuse Stokes reflection matrix through the explicit numerical solution of the vector radiative transfer equation;
3. the computation of the requisite characteristics of coherent backscattering in the exact backscattering direction from the diffuse Stokes reflection matrix;
4. the computation of the circular polarization ratio.

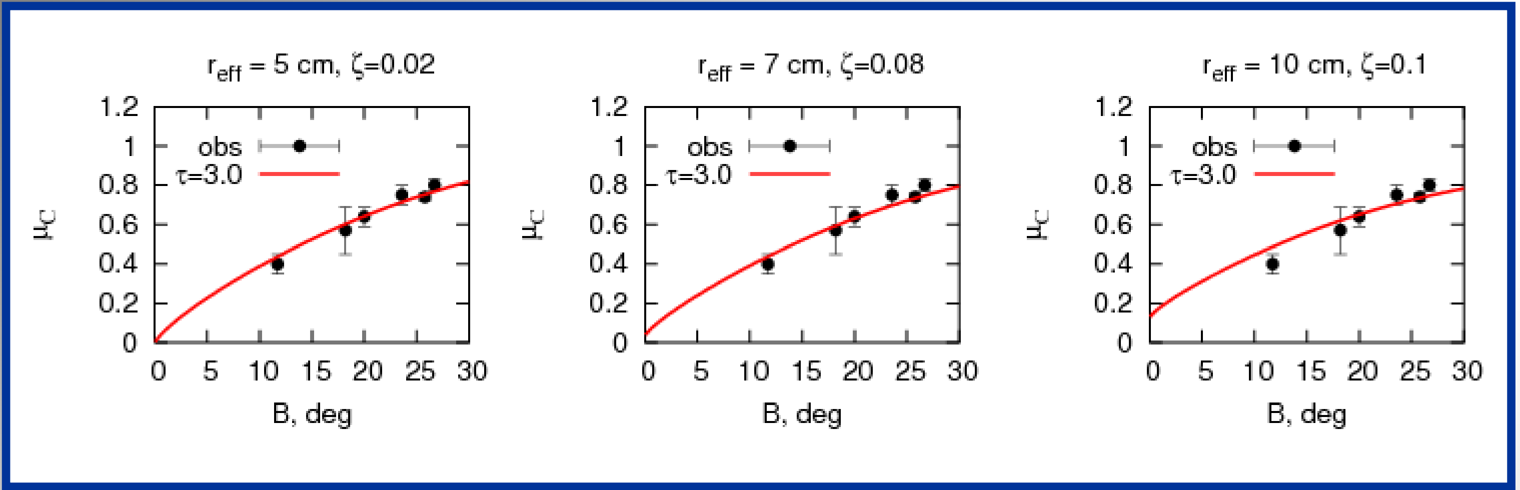

Circular polarization ratio versus ring opening angle for a plane-parallel layer consisting of polydisperse, randomly oriented Chebyshev particles (Mishchenko&Dlugach (2008)).

Conclusion

Our results favor the model of ring bodies composed of particles with small-scale surface roughness (Chebyshev particles with ς < 0.15), effective radii in the range 4 – 10 cm, and optical thickness in the range 2-3 or even larger. It is impossible to reproduce the results of radar observations without an explicit inclusion of the effect of coherent backscattering.

IV. Light scattering by densely packed random particulate media

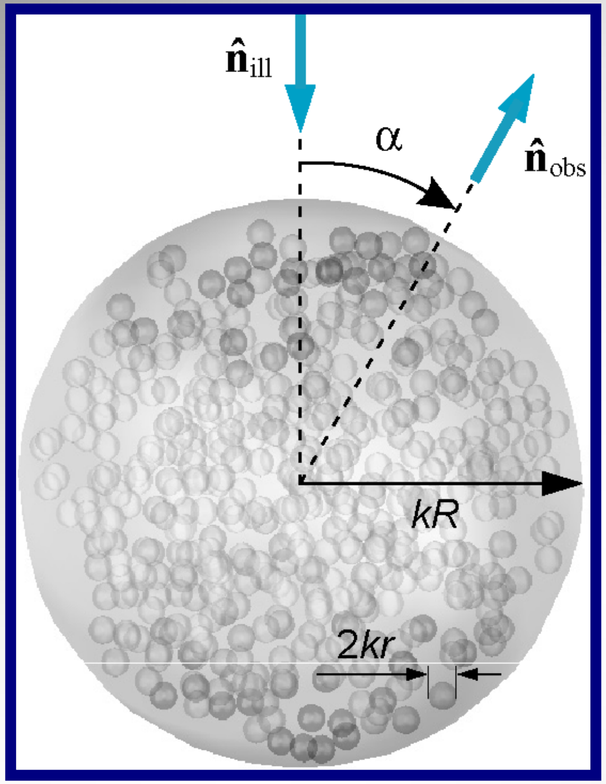

$$
\begin{bmatrix} I^{sca} \\ Q^{sca} \\ U^{sca} \\ V^{sca} \end{bmatrix} \propto \begin{bmatrix} a_1(\theta) & b_1(\theta) & 0 & 0 \\ b_1(\theta) & a_2(\theta) & 0 & 0 \\ 0 & 0 & a_3(\theta) & b_2(\theta) \\ 0 & 0 & -b_2(\theta) & a_4(\theta) \end{bmatrix} \begin{bmatrix} I^{inc} \\ Q^{inc} \\ U^{inc} \\ V^{inc} \end{bmatrix}
$$

Computational technique: the numerically exact superposition T-matrix method and the Fortran-90 multiple sphere T-matrix code developed by Mackowski for use on parallel computer clusters.

http://www.eng.auburn.edu/users/dmckwski/scatcodes

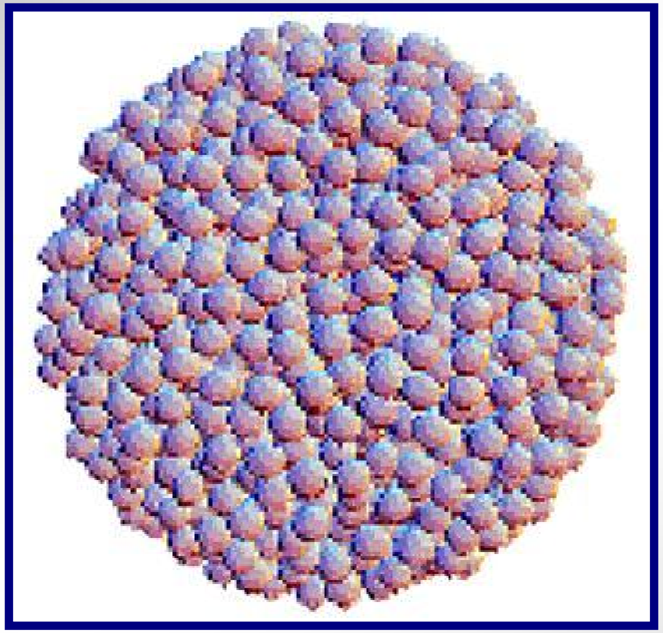

N = 1875, m = 1.31, kR = 31, kr = 2, ρ = 0.5
(Mackowski&Mishchenko 2011)

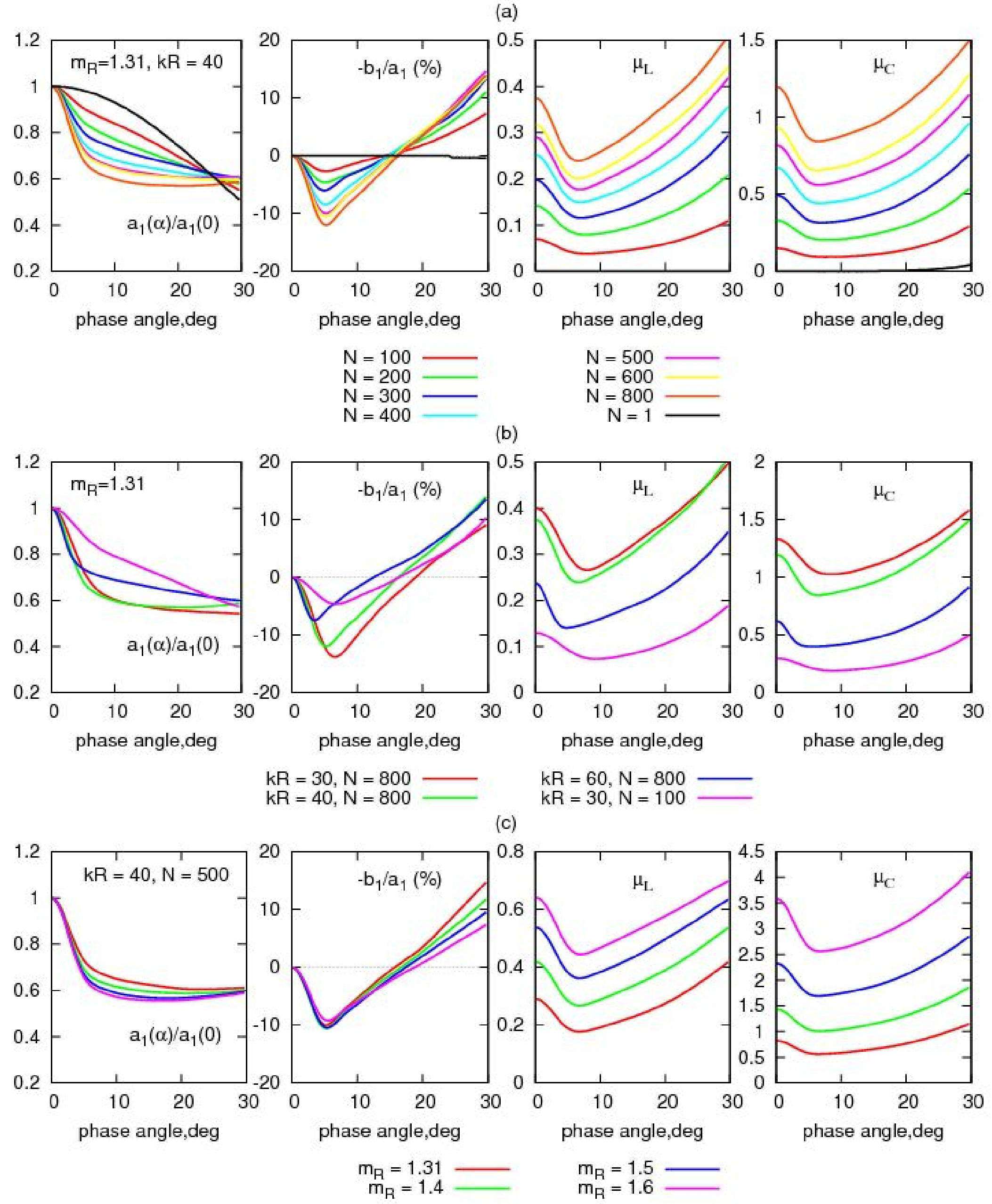

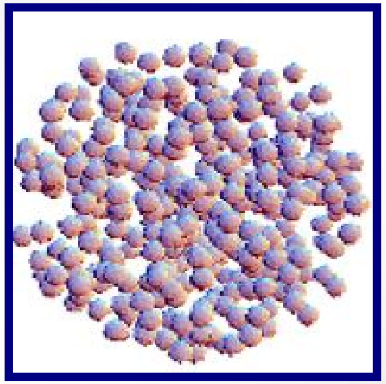

Backscattering characteristics of scattering volumes of different values of size parameter *kR* filled with different number *N* of spherical particles of different refractive index *m* (Dlugach, Mishchenko, Liu, Mackowski (2011)).

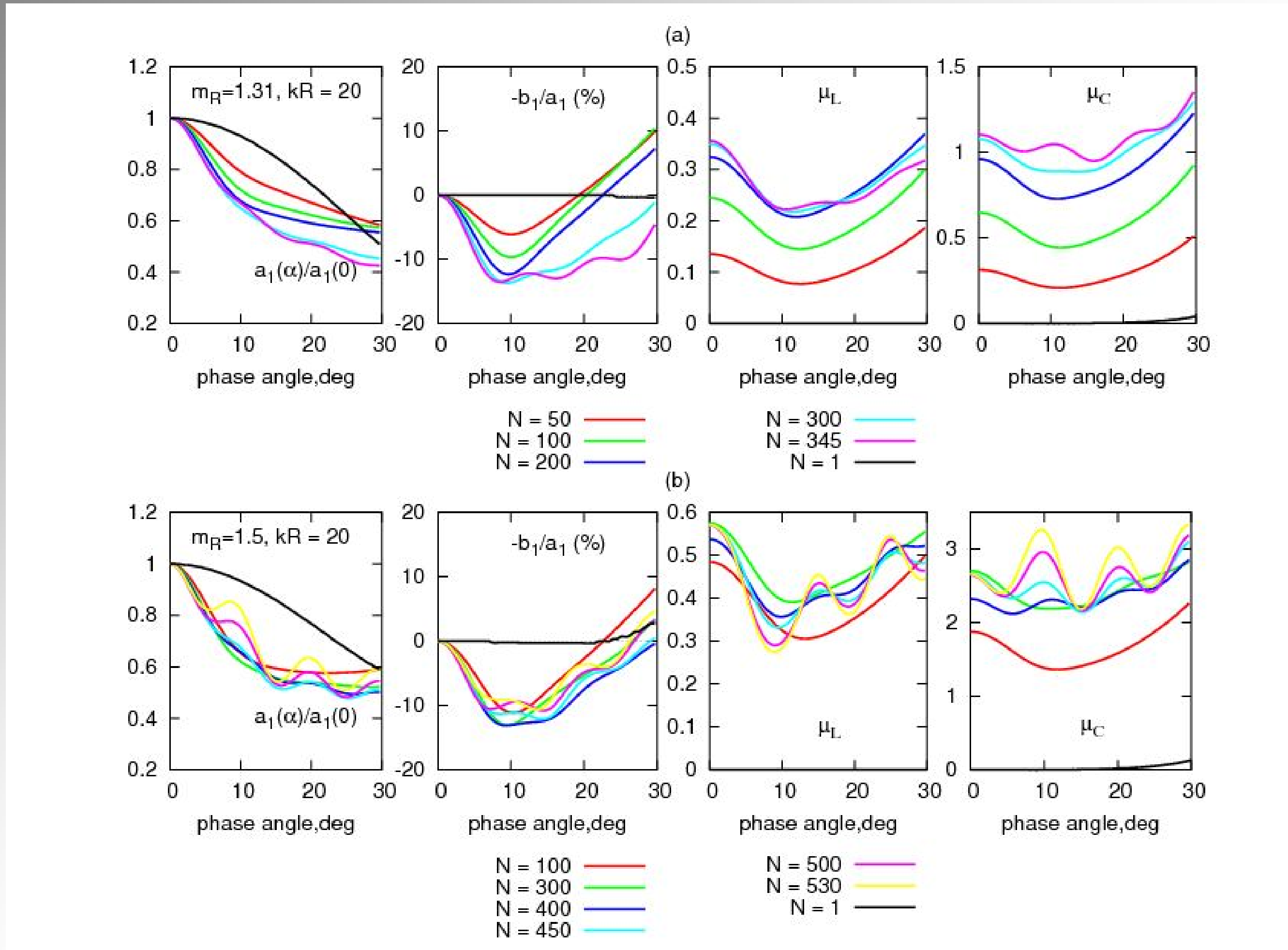

Optical characteristics of *kR* = 20 scattering volumes randomly filled with different number *N* of scattering particles with *m* = 1.31 and 1.5 (Dlugach, Mishchenko, Liu, Mackowski (2011)).

Conclusion

-All backscattering effects predicted by the low-density theory of coherent backscattering also can take place in the case of a densely packed medium.

- In the case of exceedingly large values of the particle packing density, the scattering characteristics show behavior, which is not predicted by the low density theories. Nevertheless, the direct solutions of the Maxwell equations do demonstrate that the classical predictions of the low-density theories can survive (at least in a semi-quantitative sense) volume packing densities typical of particle suspensions and particulate surfaces.

V. Opposition effects in some atmosphereless solar system bodies

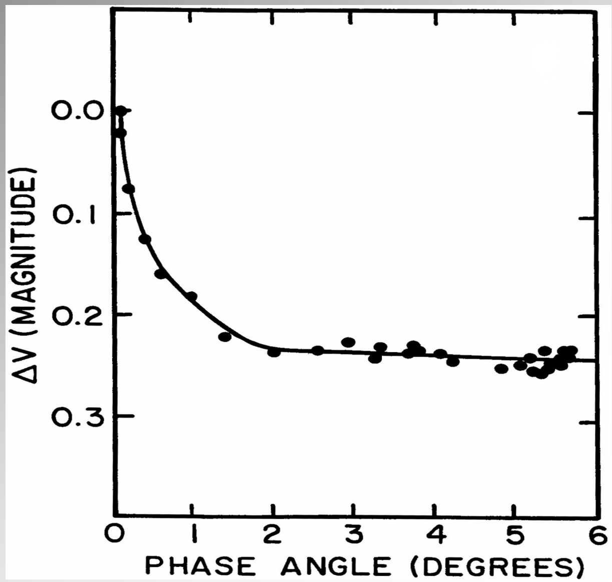

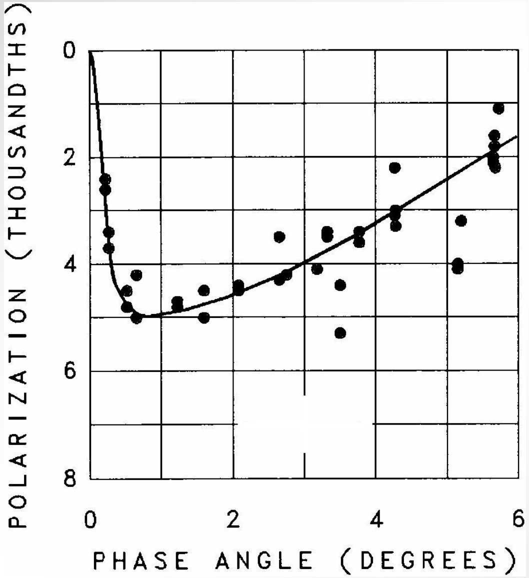

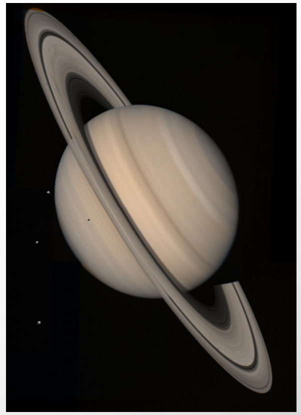

Saturn's rings

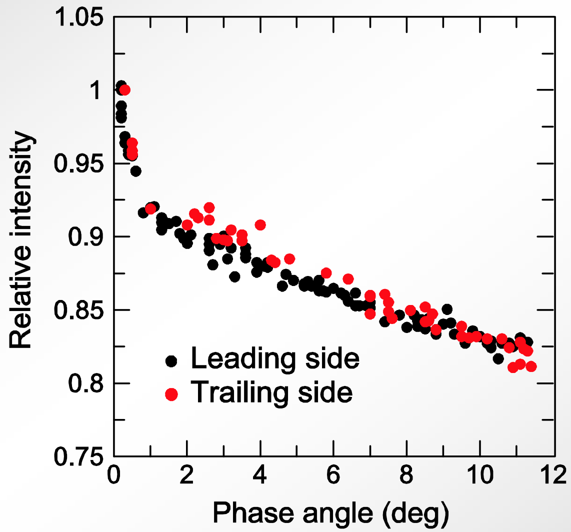

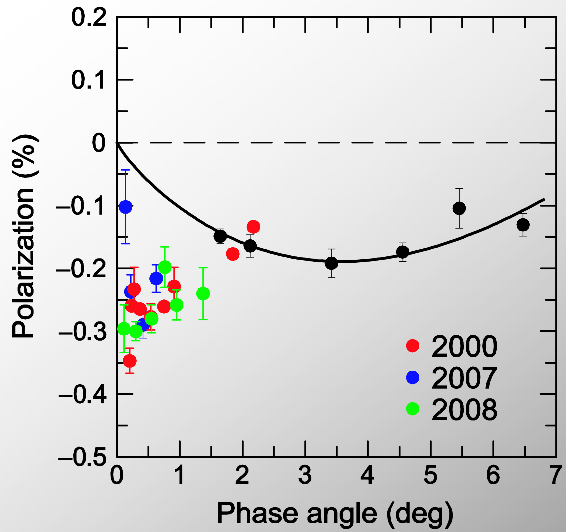

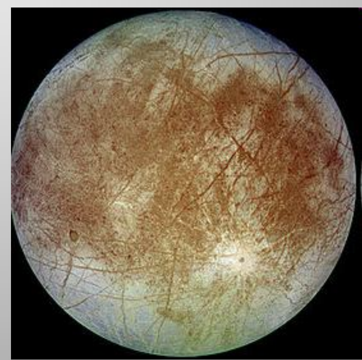

Europe

Conclusion

- The photometric and polarimetric observational data for several high-albedo solar system objects reveal simultaneous brightness and polarization opposition effects of nearly equal angular widths and with angular profiles consistent with the exact solutions of the Maxwell equations.

- So far no other rigorous theory of electromagnetic scattering has been able to reproduce both effects with their very specific traits simultaneously. Therefore, the results of our theoretical analysis point to the conclusion that both brightness and polarization opposition effects are caused by the coherent backscattering of sunlight by regolith layers composed of microscopic grains.

Acknowledgments

J. Dlugach appreciates a financial support from the Local Organizing Committee. This research was partially sponsored by the NASA Radiation Sciences Program managed by Hal Maring and by the NASA Remote Sensing Theory Program managed by Lucia Tsaoussi. We acknowledge support from the National Academy of Sciences of Ukraine under the Main Astronomical Observatory GRAPE/GPU/GRID Computer Cluster Project.

Thank you for your attention!